






High speed superconducting nanowire single-photon detector with nine interleaved nanowires

Jia Huang^{1,2,3} , Weijun Zhang^{1,3,4} , Lixing You^{1,3,4} , Chengjun Zhang^{1,2,3},
Chaolin Lv^{1,2,3} , Yong Wang^{1,2,3}, Xiaoyu Liu^{1,3}, Hao Li^{1,3}  and
Zhen Wang^{1,3}

¹ State Key Laboratory of Functional Materials for Informatics, Shanghai Institute of Microsystem and Information Technology (SIMIT), Chinese Academy of Sciences, 865 Changning Rd., Shanghai 200050, People's Republic of China

² University of Chinese Academy of Sciences, 19A Yuquan Rd., Beijing 100049, People's Republic of China

³ CAS Center for Excellence in Superconducting Electronics (CENSE), Shanghai 200050, People's Republic of China

E-mail: zhangweijun@mail.sim.ac.cn and lxyou@mail.sim.ac.cn

Received 1 April 2018, revised 26 April 2018

Accepted for publication 1 May 2018

Published 18 May 2018



Abstract

Count rate (CR) is one of the key parameters of superconducting nanowire single-photon detectors (SNSPDs). The practical SNSPDs usually have a CR of a few MHz to a few tens of MHz owing to the large kinetic inductance originating from the long nanowire, which is necessary for effectively coupling the photons. A feasible approach to decrease the kinetic inductance and consequently increase the detection speed is to replace a long single nanowire with multiple individual nanowires in an array. In this study, we report an SNSPD of nine interleaved nanowires with 70% system detection efficiency (SDE) and 200 Hz dark count rate at the low-photon-flux limit of 1550 nm. Owing to the small dead time (<6 ns) of each nanowire, the SNSPD achieved a maximum CR of 0.93 GHz at a photon flux of 1.26×10^{10} photons s^{-1} with an SDE of $\sim 7.4\%$, and a CR of 200 MHz with an SDE of over 50%. Furthermore, a photon number resolvability of up to nine photons was also demonstrated.

Keywords: single-photon detector, superconducting nanowire, count rate, photon number resolvability, detection efficiency

(Some figures may appear in colour only in the online journal)

1. Introduction

Superconducting nanowire single-photon detectors (SNSPDs) have emerged with distinguished performance parameters and various interesting applications, including quantum key distribution (QKD) [1], deep space optical communication (DSOC) [2], spectroscopy [3], quantum fingerprinting [4], and laser ranging and imaging [5, 6]. Fiber-coupled SNSPDs operate with a system detection efficiency (SDE) of $\sim 90\%$ at 1550 nm and have been obtained using WSi, NbN, and MoSi

ultrathin films [7–9]. A sub-nanosecond dead time has also been reported for a waveguide-coupled SNSPD [10]. Low dark count rate (DCR) [11–14] and low timing jitter [15–17] SNSPDs have also been fabricated in other studies. Though SNSPDs do not intrinsically have photon number resolvability (PNR), SNSPDs based on nanowires arranged in a series configuration showed PNR of up to 24 photons [18]. Challenges exist for combining some or all of the parameters mentioned above in a single SNSPD; however interest in this field of study has been growing recently [19, 20]. Research on the trade-off between SDE and CR is of particular interest. Though SNSPDs have the potential to realize a count rate of

⁴ Authors to whom any correspondence should be addressed.

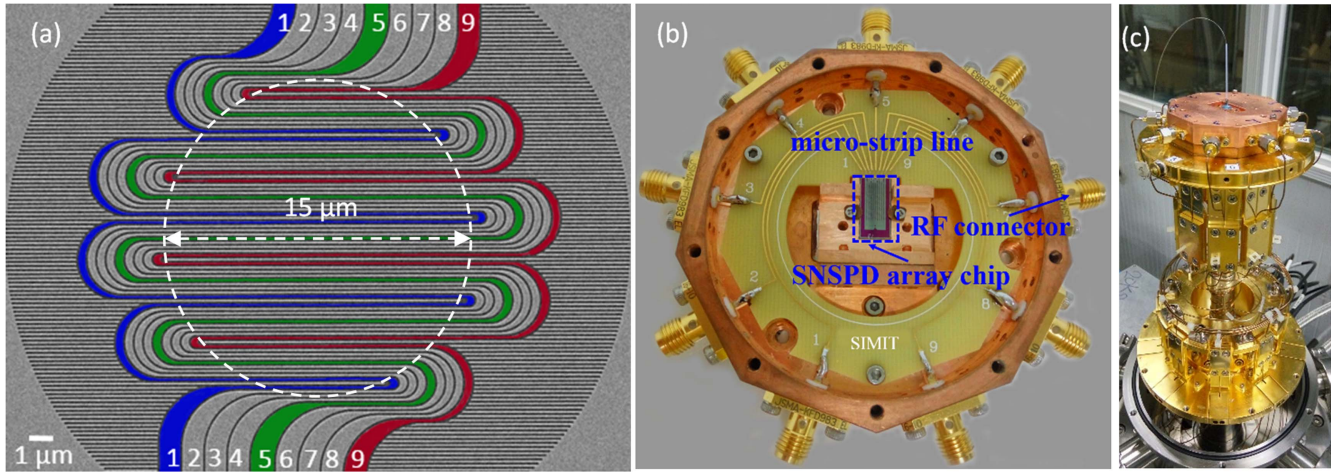


Figure 1. (a) SEM image of a nine interleaved nanowire SNSPD array (active area of 15 μm in diameter as denoted by the dashed circle), pseudo-colors in blue, green and red were used to indicate three of the nine nanowires. (b) Photo of the chip-mounting block holding the SNSPD chip. (c) Photo of the GM cryocooler system with the packaged SNSPD array without the three shielding layers.

tens of GHz, as estimated from the thermal relaxation time of tens of picoseconds [21, 22], in practice, SNSPDs usually have a CR of the order of a few MHz to a few tens of MHz owing to high kinetic inductance, which originates from the long nanowire necessary for effectively coupling the photons from the fiber.

A feasible method to decrease the kinetic inductance (and to increase the CR), while keeping the same effective active area, is to replace a long single nanowire with multi-interleaved nanowires [23]. The multi-interleaved nanowires form an SNSPD array by sharing the same active area. Each nanowire functions as an independently biased SNSPD, thus allowing high speed and photon number resolution without sacrificing SDE. Such a device would be interesting for applications, such as high speed QKD and long-distance optical communications. In 2013, Rosenberg *et al* reported a four-interleaved nanowire NbN SNSPD array with a CR of 68 MHz, an SDE of 68% at 1550 nm with $\sim\text{kHz}$ noise, and a PNR of four photons [24]. Similar SNSPDs operated successfully in the lunar laser communication demonstration with downlink data rates of up to 622 Mb s⁻¹ [25]. Recently, a free-space coupled WSi SNSPD array of 64 interleaved nanowires was developed for the DSOC application, and an SDE of 40%, a maximum CR of ~ 1.2 GHz and a timing jitter per nanowire of ~ 115 ps while being operated at ~ 500 mK was achieved [2].

In this study, we report on a nine interleaved nanowire NbN SNSPD array with a circular active area of 15 μm in diameter fabricated on a thermally oxidized Si substrate for the 1550 nm wavelength. The SNSPD was installed onto a Gifford–McMahon (GM) cryocooler with a base temperature of 2.2 K. The main performance parameters of the SNSPD array are listed as follows: an SDE of 70% at a photon flux of 10^5 s^{-1} , a maximum CR of 0.93 GHz at a photon flux of $1.26 \times 10^{10} \text{ photons s}^{-1}$ (with an SDE of $\sim 7.4\%$), a dead time below 6 ns and a timing jitter of less than 50 ps per nanowire. In addition, a PNR of nine photons was also recorded.

2. Device design and experimental setup

Figure 1(a) shows the scanning electron microscope image of a fabricated device. The device comprised nine interleaved nanowires forming a circular active area of 15 μm in diameter. The bends of each nanowire were rounded to minimize the current crowding effect [26, 27]. This nine-nanowire SNSPD array effectively decreases the length of each nanowire (i.e. smaller kinetic inductance) compared with a single nanowire SNSPD that exhibits the same active area. Moreover, the interleaved design ensures that all nanowires are illuminated equally, which enables a higher CR and a better PNR compared with a spatial array of multiple nanowires [28]. The device was fabricated from a 6.5 nm thick NbN film, which was magnetron sputtered onto a 400 μm thick thermally oxidized Si wafer (268 nm thick SiO₂ layers on both sides). The NbN film was then patterned by electron beam lithography and reactive ion etching into nanowires, each with a 90 nm line width and a 200 nm pitch. A quarter-wave optical stack with a 210 nm thick SiO layer and a metallic mirror (comprising with 5 nm of Ti and 100 nm of Au) was deposited on the nanowires to enhance the photon absorption at 1550 nm. After fabrication, the SNSPD array was aligned with a single-mode lens fiber on the backside at room temperature. Each nanowire of the array was bonded to a micro-strip line and subsequently soldered to an SMA connector. The chip-mounting block was mounted and then cooled down to 2.2 K in a closed-cycle GM cryocooler. Figure 1(b) shows the chip-mounting block for the nine-nanowire SNSPD array. Figure 1(c) shows the block installed onto the cryocooler without the three radiation shields. Each nanowire was biased separately and read via individual cryogenic coaxial cables and room temperature circuits. To reduce the blackbody radiation, the optical fiber was attached to the SNSPD package and coiled at a low temperature with a radius of 3 cm [29].

The schematic of the experimental setup is shown in figure 2. The intensity of photons emitted from the

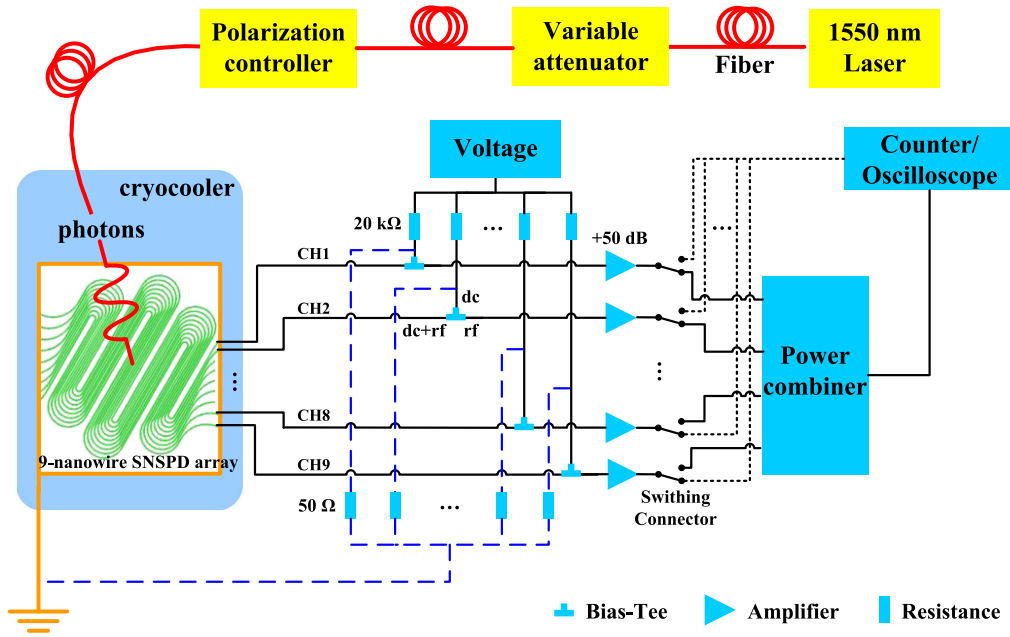


Figure 2. Schematic showing the experimental setup used to characterize the SNSPD array.

continuous-wave or pulsed laser, which could be tuned by serial variable attenuators. Polarization was adjusted by a polarization controller to obtain the maximum SDE. Finally, the polarized photons were illuminated onto the SNSPD through a single-mode optical fiber. Each nanowire was biased and read out either simultaneously or individually. The voltage pulse generated from each nanowire of the SNSPD array was amplified using a room temperature 50 dB low noise amplifier (RF Bay Inc., LNA-650). The output signals were monitored either using a high speed oscilloscope (Keysight, DSO-V 334A) or photon counters (SRS Inc., SR400). By switching the connection of the readout components outside the cryocooler system, we can characterize each nanowire (as shown by the black dotted lines). A commercial power combiner was employed to combine the amplified signals of all nine channels into a single output to characterize the total performance.

3. Results

We characterized SNSPD arrays with three different active areas (10, 15, and 20 μm in diameter) fabricated on the same 2 inch wafer. Figure 3 displays the normalized output pulses for a single nanowire of the arrays with different-sized active areas. For active areas with diameters of 10, 15, and 20 μm , the dead times (τ_d , defined as the time at which the height of the pulse is reduced to $1/e = 0.368$ of its initial value) of each single nanowire, as obtained from the exponential fits, were about 3.3, 5.6, and 7.9 ns, respectively. The inset in figure 3 shows the switching currents, I_{sw} , for all nine nanowires within the 15 μm device, the small deviation ($13.04 \pm 0.29 \mu\text{A}$) indicates that all nanowires were fabricated with high uniformity. To reach a trade-off between effective optical coupling and high speed, the SNSPD array

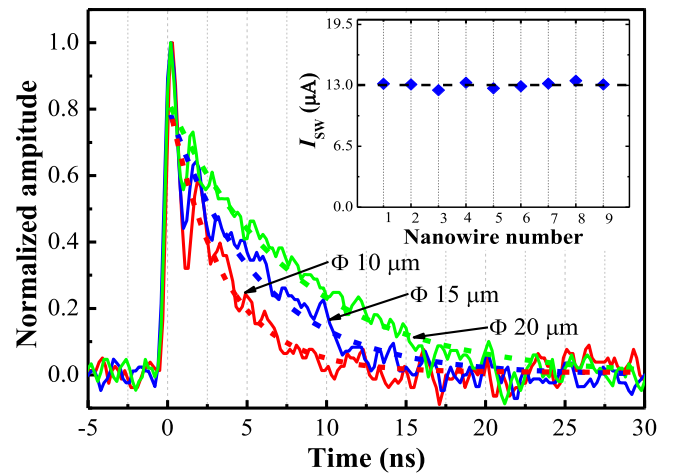


Figure 3. Normalized output pulses of nanowires of the SNSPD arrays with different active areas at a bias of $0.9 I_{sw}$. The exponential fits of the falling edges are displayed as dashed lines. The red, blue and green lines represent SNSPD arrays for active areas with diameters of 10, 15, and 20 μm , respectively. Excluding the active area of the array, the three nanowires have the same parameters (thickness of 6.5 nm, line width of 90 nm, gap width of 110 nm); the inset shows the plot of I_{sw} for the nine nanowires from the 15 μm diameter active area SNSPD array (mean value (blue dotted line) and standard deviations of $13.04 \mu\text{A}$ and $0.29 \mu\text{A}$, respectively).

with an active area of 15 μm in diameter was studied with the following experiments and results.

To measure the SDE and DCR as functions of the bias current, photons emitted by a continuous-wave tunable laser (Keysight, 81970A) were attenuated to $10^5 \text{ photons s}^{-1}$ using variable attenuators. The SDE was calculated using the following formula: $\text{SDE} = (\text{OPR} - \text{DCR})/\text{PR}$, where OPR is the output pulse CR and PR is the total photon input rate to the system. The DCR was measured when the optical input of the system is blocked. At each bias current, OPR and DCR

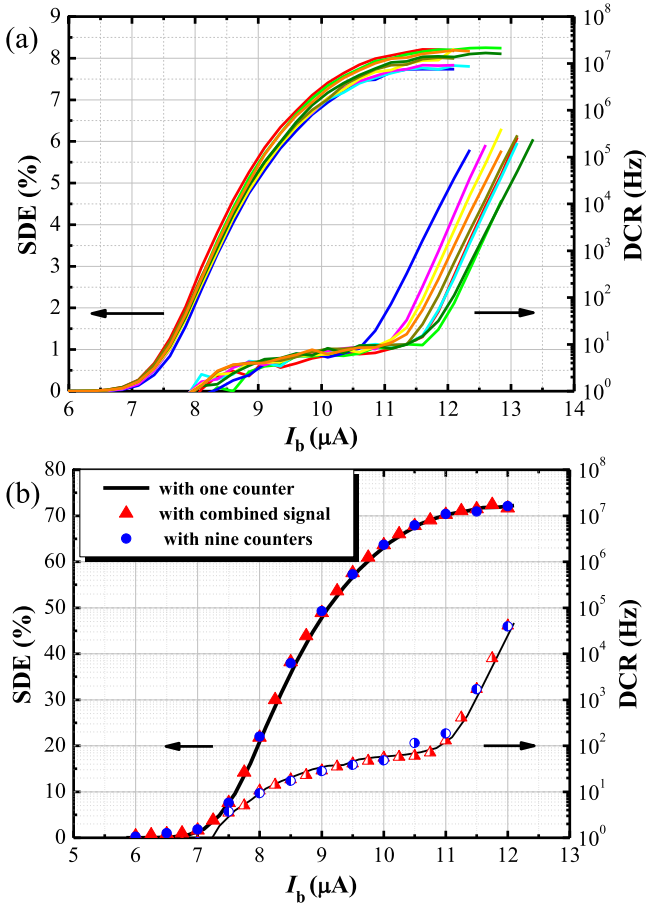


Figure 4. SDE and DCR as function of the bias current recorded as (a) nine single nanowires and (b) the sum of the nine nanowires.

were collected for 10 s. Figure 4(a) shows the SDE and DCR as a function of the bias current for each nanowire. The SDE curve of each nanowire is saturated, and the maximum SDEs exhibit a small distribution range between 7.8% and 8.2%. Figure 4(b) shows the total SDE and DCR summed over the nine nanowires, the data was obtained via the following three approaches: (i) Record the counts in succession using a single counter by switching the RF connection to the individual nanowire and subsequently summing the counts (see the 'black line'). (ii) Read out the nine nanowires simultaneously by nine counter channels and then sum the counts (see the 'blue scatters'). (iii) Use a power combiner to combine the nine-nanowire signals into a single channel, and then count the combined signals (see the 'red triangles'). The results of the three methods were found to be consistent with each other, which indicated negligible crosstalk among the channels. The total SDE reached a maximum value of 70.3% at a total DCR of ~ 200 Hz when all of the nanowires were biased at 11 μA.

High CR is one of the key merits of a multi-interleaved nanowire SNSPD array when it operates as a single detector. Figure 5(a) shows the CR as a function of the input photon rate for a single nanowire, measured by two methods with and without a 50 ohm shunt resistor, inserted between the dc arm of the bias tee and the ground at room temperature (indicated with blue dashed lines in figure 2). Without a 50 ohm shunt

resistor, the CR of a single nanowire only reached a maximum of ~ 10 MHz as increasing the bias resulted in latching. However, with a 50 ohm shunt resistor, the bias scheme worked as a quasi-constant voltage bias to the SNSPD, which then enabled the device to avoid the latching [30]. Consequently, we can obtain a maximum CR of up to ~ 100 MHz per nanowire. At low-photon intensities in both cases, the CR of the device increases linearly with the number of incident photons. When the input photon rate is high (> 20 MHz), nonlinearity is observed owing to the limitation of the AC coupled readout circuit [31]. We expect that further CR improvements can be achieved using a new readout circuit and other approaches in future [32]. Figure 5(b) shows the dependence of the normalized SDE on CR for a single nanowire (blue line) and the array (red line) when the shunt resistor is adopted. The SDE for the array was acquired from the summed counts of the nine nanowires recorded simultaneously by nine channels of counters. A picosecond-pulsed laser (Hamamatsu Inc., C10196) with a repetitive rate of 1 GHz was applied as the light source. The biased currents of the nine nanowires were fixed at the same value with a total DCR of ~ 200 Hz. We achieved a total CR of 275 MHz with a SDE of $\sim 50\%$, and the CR_{exp} (the CR where the SDE was a $1/e$ expression of its maximum value) was found to be ~ 600 MHz. The detector array could count photons at a high rate with the further sacrifice of the SDE. For example, we obtained a CR of 0.928 GHz with a SDE of $\sim 7.4\%$ for an incident photon rate of ~ 12.6 GHz.

By combining the output signal of the nine nanowires using the power combiner, we were able to demonstrate the PNR of the SNSPD array. The signal was acquired by an 80 GHz sampling oscilloscope (Keysight, DSO-V 334A). A femtosecond-pulsed laser (Calmar, FPL-01CAF) was used as the light source with a repetition rate of 20 MHz. The average input photon number was attenuated to 15 photons/pulse. Figure 6(a) shows a single-shot oscilloscope trace of the combined signal, nine distinct pulse heights are clearly distinguishable from the amplitude of the pulses, which correspond to the detection of one to nine photons. The base line below zero is known to be caused by the AC coupled readout circuit, as discussed in a previous report [32]. The histograms of the pulse height distribution were also obtained by sampling the CRs of the photo-responses with different amplitudes, which were fitted well by a sum of the Gaussian peaks, as shown in figure 6(b).

Figure 7 shows the timing resolution of the nine-nanowire SNSPD array. A femtosecond-pulsed laser (Calmar, FPL-01CAF) with a sub-ps timing jitter (T_j) was used as the light source [20]. The system T_j was measured using a timing-correlated photon counting module [33]. Figure 7(a) displays the bias current dependence of T_j s for each single nanowire and also the total bias current dependence for all nine nanowires (output signal of the power combiner), the input photon flux was attenuated to the single-photon level in both cases. The T_j decreased as the bias current increased, which implied that the signal-to-noise ratio plays a key role in determining the T_j . The T_j of a single nanowire was less than 50 ps when biased at 11 μA, while the measured total T_j was about

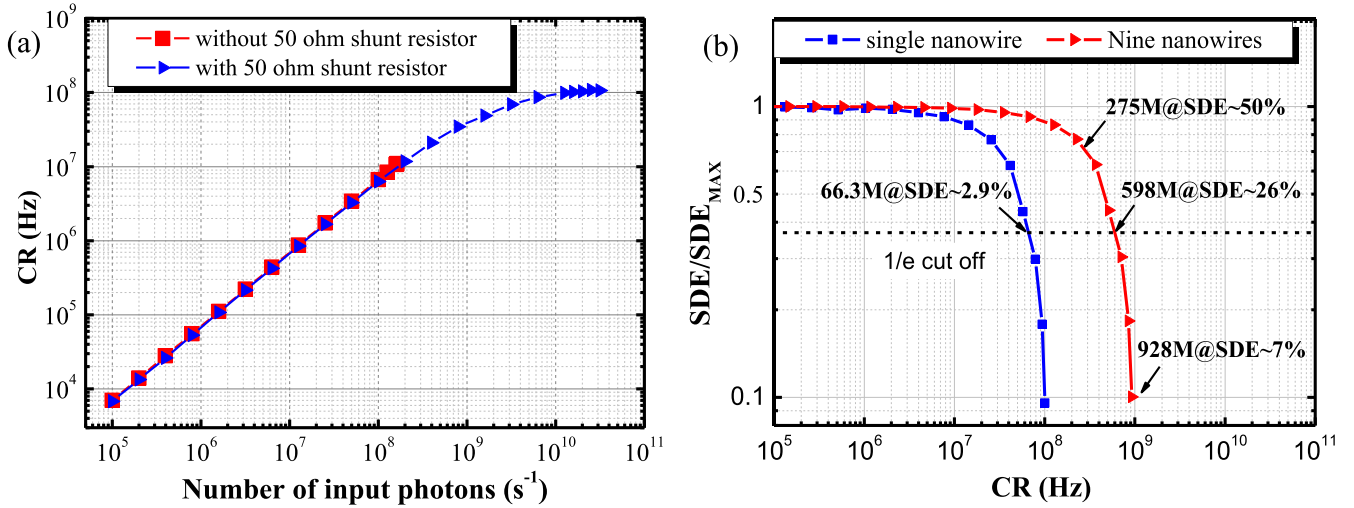


Figure 5. (a) Measured count rates of a single nanowire versus input photons s^{-1} . The blue and red scatter plots correspond to the results of the same nanowire with and without a 50 ohm shunt resistor at room temperature, when the nanowire was biased at a DCR of 10 Hz. The 50 ohm shunt resistor was inserted between the dc arm of the bias tee and the ground at room temperature. (b) Dependence of an individual and the total SDEs (normalized) on the measured CR with a 50 ohm shunt resistor. The blue curve represents the result of the single nanowire, while the red curve is the CR obtained by summing over nine nanowires.

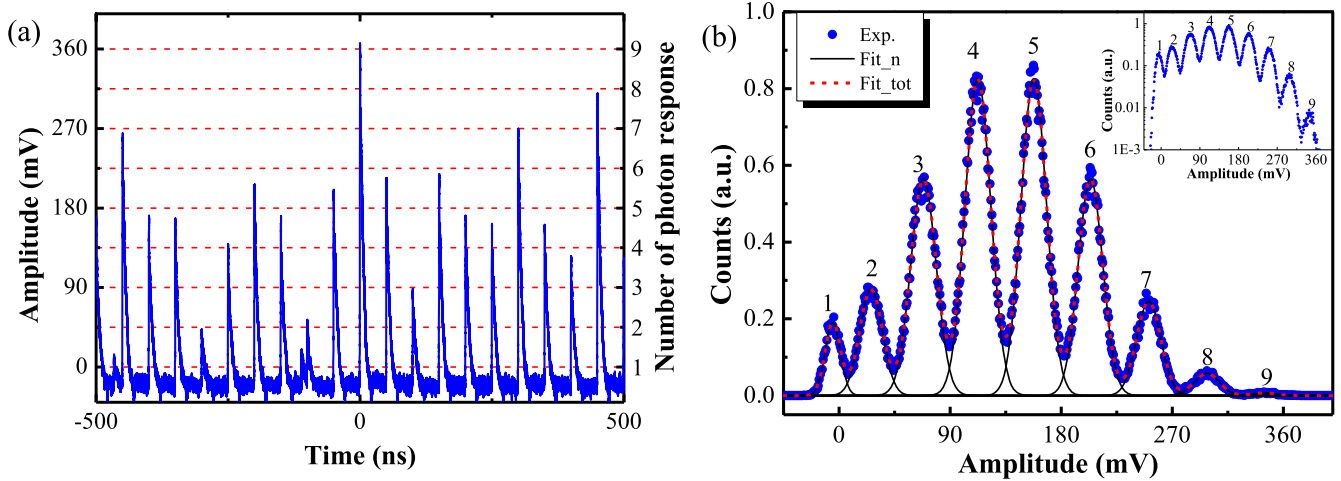


Figure 6. (a) Single-shot oscilloscope trace of a nine-nanowire SNSPD array; nine distinct pulse heights are clearly distinguishable. (b) Experimental (blue circle) and fitted-line (black solid and red dashed) of the pulse height distribution. The single Gaussian fits (Fit_n) are shown as solid black lines, and their sum (Fit_tot) is depicted as a dashed red line. The inset shows the height distributions in logarithmic coordinates.

176 ps, which was larger than a calculated value (T_{jc}) of 127 ps. The T_{jc} was calculated by using an expression of $\sqrt{\sum_{i=1}^9 T_{ji}^2}$, where T_{ji} denotes the measured T_j of i th-nanowire at $11 \mu\text{A}$, assuming the T_{ji} is independent. Here are two possible explanations for this deviation. One is that the reduced signal-to-noise ratio of about 1.7 dB was caused by the power combiner; the other is that an asynchronous signal is received from the nine nanowires (mainly caused by slight differences in coaxial cables length and connection ports). Figure 7(b) shows the T_j measurement when the device was biased at $11 \mu\text{A}$. The inset of figure 7(b) displays the T_j of a single nanowire as a function of the number of photons/pulse, which indicates that T_j does not vary with increasing photon intensity. Owing to the high signal-to-noise ratio of the nine-photon response signal (the output signal amplitude is

~ 360 mV and the threshold voltage is 337 mV), the T_j value defined by the full width at half maximum of the histogram was 24.9 ps.

4. Discussion

Further work can be done to enhance the merits of interleaved SNSPD. For examples, first, by improving the optical coupling and through material optimization, the SDE can be increased further to its maximum absorptance ($>90\%$). Second, the DCR can be suppressed by integrating a bandpass filter into the chip or on the face of the fiber end [12, 34]. Besides, as a result of the conventional circuit readout, the maximum CR of the device was limited. However, the

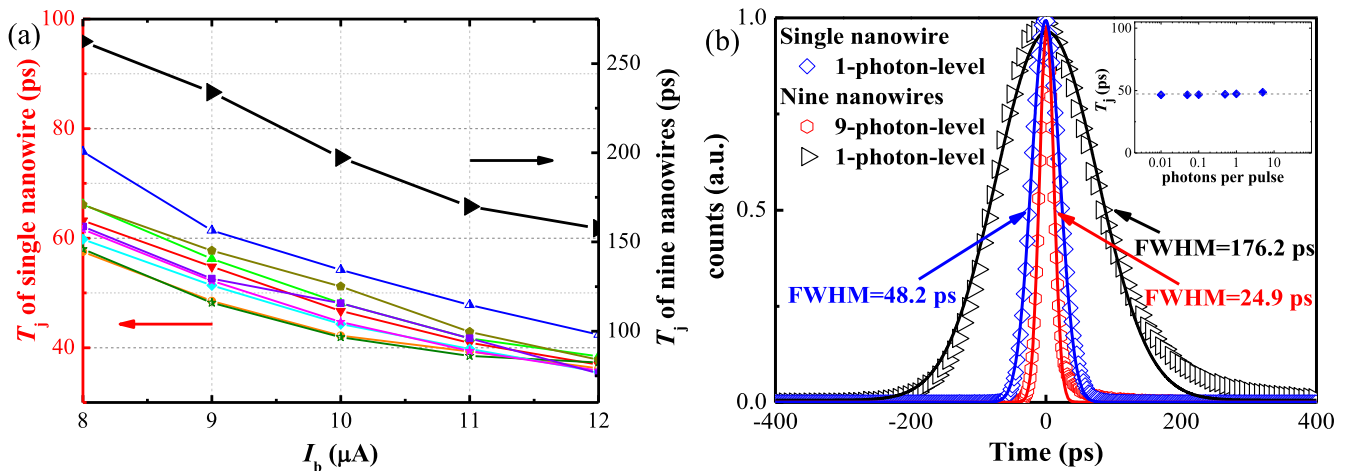


Figure 7. Timing jitters of the nine-nanowire SNSPD array. (a) Bias current dependence of T_j , the colored symbols and lines represent the T_j s of nine different nanowires, while the black symbol and line displays the T_j of the array. Biased at 11 μ A, the measured T_j of the single nanowire was 41.9, 40.3, 39.5, 40.8, 40.4, 42.7, 48.2, 43.9, and 42.7 ps, respectively. (b) T_j measurement when the device was biased at 11 μ A. The blue scatter plot represents the T_j of one of the nanowires under single-photon level illumination, while the black and red scatter plots show T_j of nine nanowires under two different threshold levels: nine-photon level (337 mV) and single-photon level (23 mV). The input photon flux was attenuated to 15 photons/pulse at the nine-photon level and to 0.01 photons/pulse for the single-photon level. The inset displays the T_j of a single nanowire as a function of photons/pulse.

maximum CR could exceed GHz level by introducing a DC-coupled readout circuit or capacitor-grounded readout circuit [31, 32], etc. Moreover, the PNR fidelity can be effectively increased by further improving the SDE and increasing the number of interleaved nanowires [23].

5. Conclusions

In this work, we designed, fabricated, and measured an SNSPD array with nine interleaved nanowires. At 1550 nm, our nine-nanowire SNSPD array reached an SDE of 70% at a DCR of 200 Hz at the low-photon-flux limit. We obtained a CR of 275 MHz with an SDE of \sim 50%, and a maximum CR of 0.93 GHz with an SDE of \sim 7%. The device was able to resolve up to nine photons. Our SNSPD array with high speed, efficiency, and PNR will have prospective applications in fields, such as space-based quantum communication, laser ranging, and single-photon imaging.

Acknowledgments

This work is supported by the National Key R&D Program of China (2017YFA0304000), the Science and Technology Commission of Shanghai Municipality under Grant (16JC1400402) and Program of Shanghai Academic/Technology Research Leader under Grant (18XD1404600).

ORCID iDs

Jia Huang <https://orcid.org/0000-0003-0693-6558>
 Weijun Zhang <https://orcid.org/0000-0002-9432-7404>
 Lixing You <https://orcid.org/0000-0001-7304-0474>

Chaolin Lv <https://orcid.org/0000-0003-4343-4071>
 Hao Li <https://orcid.org/0000-0001-6946-4362>

References

- [1] Yin H-L *et al* 2016 Measurement-device-independent quantum key distribution over a 404 km optical fiber *Phys. Rev. Lett.* **117** 190501
- [2] Allmaras J P *et al* 2017 Large-area 64 pixel array of WSi superconducting nanowire single photon detectors *Conf. on Lasers and Electro-Optics* (Washington, DC: Optical Society of America) JTh3E.7 (https://doi.org/10.1364/CLEO_AT.2017.JTh3E.7)
- [3] Yamashita T, Liu D, Miki S, Yamamoto J, Haraguchi T, Kinjo M, Hiraoka Y, Wang Z and Terai H 2014 Fluorescence correlation spectroscopy with visible-wavelength superconducting nanowire single-photon detector *Opt. Express* **22** 28783
- [4] Guan J-Y *et al* 2016 Observation of quantum fingerprinting beating the classical limit *Phys. Rev. Lett.* **116** 240502
- [5] Li H, Chen S, You L, Meng W, Wu Z, Zhang Z, Tang K, Zhang L, Zhang W and Yang X 2016 Superconducting nanowire single photon detector at 532 nm and demonstration in satellite laser ranging *Opt. Express* **24** 3535
- [6] Zhou H, He Y, You L, Chen S, Zhang W, Wu J, Wang Z and Xie X 2015 Few-photon imaging at 1550 nm using a low-timing-jitter superconducting nanowire single-photon detector *Opt. Express* **23** 14603
- [7] Marsili F *et al* 2013 Detecting single infrared photons with 93% system efficiency *Nat. Photon.* **7** 210
- [8] Zhang W, You L, Li H, Huang J, Lv C, Zhang L, Liu X, Wu J, Wang Z and Xie X 2017 NbN superconducting nanowire single photon detector with efficiency over 90% at 1550 nm wavelength operational at compact cryocooler temperature *Sci. China Phys., Mech. Astron.* **60** 120314
- [9] Verma V B, Korzh B, Bussi eres F, Horansky R D, Dyer S D, Lita A E, Vayshenker I, Marsili F, Shaw M D and Zbinden H 2015 High-efficiency superconducting nanowire

- single-photon detectors fabricated from MoSi thin-films *Opt. Express* **23** 33792
- [10] Vetter A *et al* 2016 Cavity-enhanced and ultrafast superconducting single-photon detectors *Nano Lett.* **16** 7085
- [11] Shibata H, Shimizu K, Takesue H and Tokura Y 2015 Ultimate low system dark-count rate for superconducting nanowire single-photon detector *Opt. Lett.* **40** 3428
- [12] Yang X, Li H, Zhang W, You L, Zhang L, Liu X, Wang Z, Peng W, Xie X and Jiang M 2014 Superconducting nanowire single photon detector with on-chip bandpass filter *Opt. Express* **22** 16267
- [13] Kahl O, Ferrari S, Kovalyuk V, Goltsman G N, Korneev A and Pernice W H P 2015 Waveguide integrated superconducting single-photon detectors with high internal quantum efficiency at telecom wavelengths *Sci. Rep.* **5** 10941
- [14] Ejrnaes M, Parlato L, Arpaia R, Bauch T, Lombardi F, Cristiano R, Tafuri F and Pepe G P 2017 Observation of dark pulses in 10 nm thick YBCO nanostrips presenting hysteretic current voltage characteristics *Supercond. Sci. Technol.* **30** 12LT02
- [15] Wu J, You L, Chen S, Li H, He Y, Lv C, Wang Z and Xie X 2017 Improving the timing jitter of a superconducting nanowire single-photon detection system *Appl. Opt.* **56** 2195
- [16] Najafi F, Dane A, Bellei F, Zhao Q, Sunter K A, McCaughan A N and Berggren K K 2015 Fabrication process yielding saturated nanowire single-photon detectors with 24 ps jitter *IEEE J. Sel. Top. Quantum Electron.* **21** 1
- [17] Calandri N, Zhao Q, Zhu D, Dane A and Berggren K K 2016 Superconducting nanowire detector jitter limited by detector geometry *Appl. Phys. Lett.* **109** 152601
- [18] Mattioli F, Zhou Z, Gaggero A, Gaudio R, Leoni R and Fiore A 2016 Photon-counting and analog operation of a 24 pixel photon number resolving detector based on superconducting nanowires *Opt. Express* **24** 9067
- [19] Zadeh I E, Los J W N, Gourgues R B M, Steinmetz V, Bulgarini G, Dobrovolskiy S M, Zwiller V and Dorenbos S N 2017 Single-photon detectors combining high efficiency, high detection rates, and ultra-high timing resolution *APL Photonics* **2** 111301
- [20] Miki S, Yabuno M, Yamashita T and Terai H 2017 Stable, high-performance operation of a fiber-coupled superconducting nanowire avalanche photon detector *Opt. Express* **25** 6796
- [21] Il'in K S, Lindgren M, Currie M, Semenov A D, Gol'tsman G N, Sobolewski R, Cherednichenko S I and Gershenzon E M 2000 Picosecond hot-electron energy relaxation in NbN superconducting photodetectors *Appl. Phys. Lett.* **76** 2752
- [22] Zhang L *et al* 2018 Hotspot relaxation time of NbN superconducting nanowire single-photon detectors on various substrates *Sci. Rep.* **8** 1486
- [23] Dauler E A, Kerman A J, Robinson B S, Yang J K W, Voronov B, Goltsman G, Hamilton S A and Berggren K K 2009 Photon-number-resolution with sub-30 ps timing using multi-element superconducting nanowire single photon detectors *J. Mod. Opt.* **56** 364
- [24] Rosenberg D, Kerman A J, Molnar R J and Dauler E A 2013 High-speed and high-efficiency superconducting nanowire single photon detector array *Opt. Express* **21** 1440
- [25] Grein M E, Kerman A J, Dauler E A, Willis M M, Romkey B, Molnar R J, Robinson B S, Murphy D V and Boroson D M 2015 An optical receiver for the lunar laser communication demonstration based on photon-counting superconducting nanowires *Proc. SPIE* **9492** 949208
- [26] Huang J *et al* 2017 Spiral superconducting nanowire single-photon detector with efficiency over 50% at 1550 nm wavelength *Supercond. Sci. Technol.* **30** 074004
- [27] Clem J R and Berggren K K 2011 Geometry-dependent critical currents in superconducting nanocircuits *Phys. Rev. B* **84** 174510
- [28] Dauler E A, Robinson B S, Kerman A J, Yang J K W, Rosfjord K M, Anant V, Voronov B, Gol'tsman G and Berggren K K 2007 Multi-element superconducting nanowire single-photon detector *IEEE Trans. Appl. Supercond.* **17** 279
- [29] Smirnov K, Vachtomin Y, Divochiy A, Antipov A and Goltsman G 2015 Dependence of dark count rates in superconducting single photon detectors on the filtering effect of standard single mode optical fibers *Appl. Phys. Express* **8** 022501
- [30] Liu D, Chen S, You L, Wang Y, Miki S, Wang Z, Xie X and Jiang M 2012 Nonlatching superconducting nanowire single-photon detection with quasi-constant-voltage bias *Appl. Phys. Express* **5** 125202
- [31] Zhao Q, Jia T, Gu M, Wan C, Zhang L, Xu W, Kang L, Chen J and Wu P 2014 Counting rate enhancements in superconducting nanowire single-photon detectors with improved readout circuits *Opt. Lett.* **39** 1869
- [32] Kerman A J, Rosenberg D, Molnar R J and Dauler E A 2013 Readout of superconducting nanowire single-photon detectors at high count rates *J. Appl. Phys.* **113** 144511
- [33] You L *et al* 2013 Jitter analysis of a superconducting nanowire single photon detector *AIP Adv.* **3** 072135
- [34] Zhang W, Yang X, Li H, You L, Lv C, Zhang L, Zhang C, Liu X, Wang Z and Xie X 2018 Fiber-coupled superconducting nanowire single-photon detectors integrated with a bandpass filter on the fiber end-face *Supercond. Sci. Technol.* **31** 035012